FABRICATION OF THE PLANAR ANGULAR ROTATOR USING THE CMOS PROCESS

Hunglin Chen, Chienliu Chang, Kaihsiang Yen, Huiwen Huang, Jinhung Chio, Chingyi Wu, Peizen Chang*

Microsystems Laboratory, Industrial Technology Research Institute
Bldg. 52, 195, Sec.4, Chung Hsing Rd. Chutung, Hsinchu, Taiwan 310, R. O. C.
Fax:886-3-5820266 E-mail:hlchen@memsu1.iam.ntu.edu.tw

*Institute of Applied Mechanics, College of Engineering, National Taiwan University

ABSTRACT

This investigation proposes a novel planar angular rotator fabricated by the conventional CMOS process. Following the 0.6 μm SPTM (single poly triple metal) CMOS process, the device is completed by a simple post-process with maskless etching. The suspension unit rotates around its geometric center with electrostatic actuation. In addition to having a single rotatory component, 2×2 and 3×3 arrayed components are designed to have a larger rotatory angle with less actuation distance. The proposed design adopts an intelligent mechanism, including slider-crank and four-bar linkage, to permit simultaneous motion. With driving voltages of around 40 volts, the CMOS planar angular rotator could be driven. Comparing to the most common planar angular, micromotor, the design proposed herein has a shorter response time and longer life without the problems of friction and wear.

INTRODUCTION

Micro-Electro-Mechanical-Systems (MEMS) have received increasing interest in recent years. Various fabrication technologies, including LIGA, surface and bulk micromachining, have been developed to fulfill specific industrial requirements. However, the specialized processes may not automatically allow for on-chip integration of MEMS devices and integrated circuits. Therefore, developing a MEMS structure compatible with a commercial complimentary metal-oxide semiconductor (CMOS) process has also received extensive interest. Since CMOS is a mature and evolving batch technology, a significant amount of development time could be saved and effectively responding to fluctuating market demands would be easier if a CMOS compatible MEMS structure existed.

The most common planar rotator actuated in plane, micromotor, is proposed by many researchers [1]. Related applications of the micromotor include optical switches [2], microgear [3], and microenginees [4]. However, the friction [5] and wear of the micromotor would restrict response speed and lifetime. Researchers have also reported on another type of rotator operated at limited angles. The rotatory units are supported by flexure suspensions, making friction and wear problems avoidable. To employ the characterization of quick response, the mechanism is useful for the heads of hard disk devices [6]. The planar angular rotator suggested herein belongs to this latter type.

In light above developments, this work presents a planar angular rotator by the conventional CMOS process. One or arrayed rotatory units could be actuated by the electrostatic force. In addition to the benefits of actuation without wear and friction problems, the microactuator is designed to increase rotatory angles with less actuation displacement demand. This study also describes the configuration of the microactuator and the novelty of the kinetic behavior.

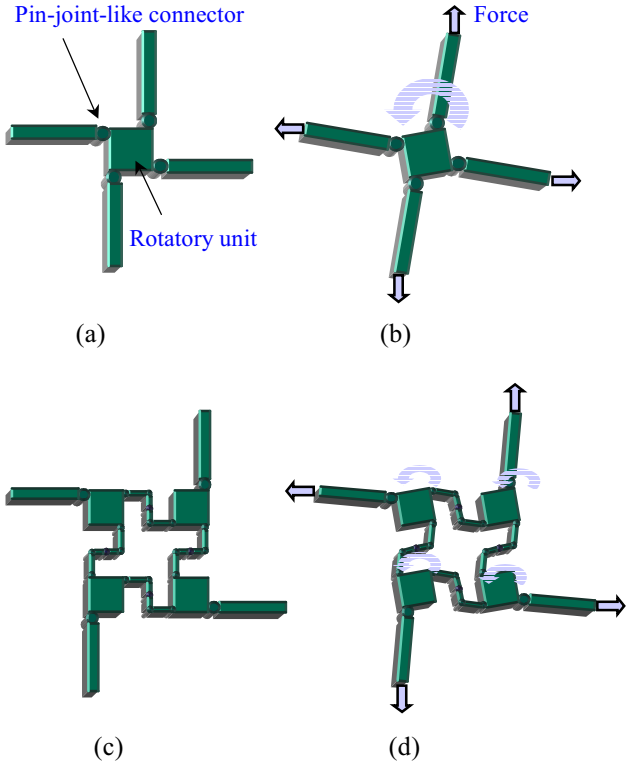

Figure 1. one and 2×2 arrayed rotatory units (b)(d)with and (a)(c)without actuation.

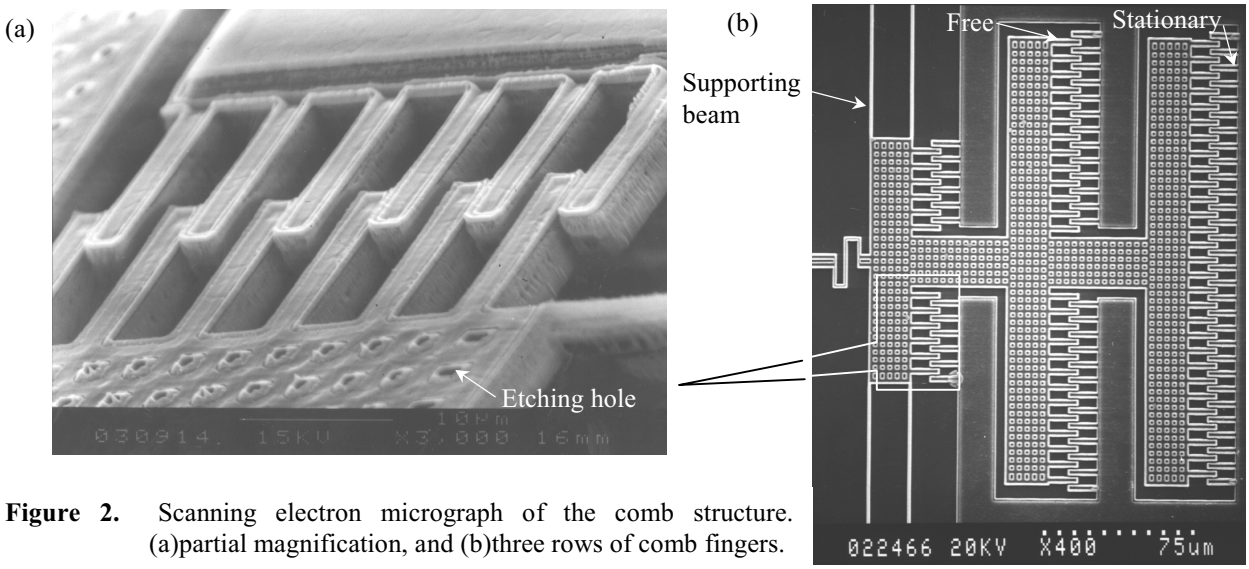

Figure 2. Scanning electron micrograph of the comb structure. (a)partial magnification, and (b)three rows of comb fingers.

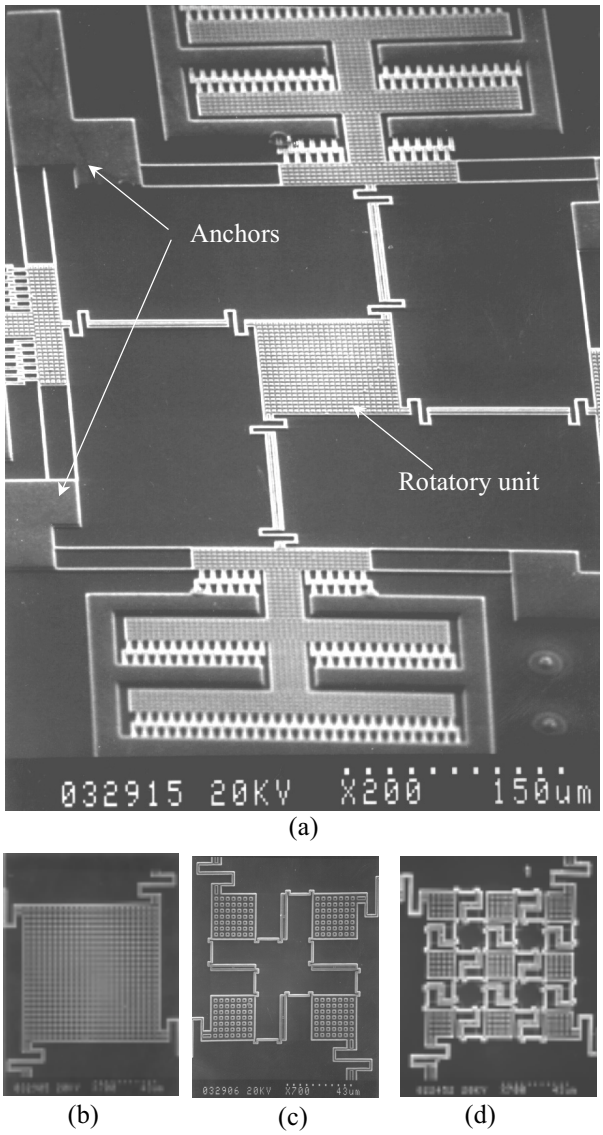

Figure 3. Scanning electron micrograph of the CMOS planar angular rotator. (a)oblique view, (b)one rotatory unit, (c)2×2 and (d)3×3 rotatory unit

OPERATING PRINCIPLE

Actuating mechanism

The actuating principle of the planar angular rotator can be derived intuitively from Fig. 1. Figure 1(a) indicates that a suspended unit is supported by four beams via the pin-joint-like [7] connectors. According to Fig. 1(b), with electrostatic force, the beams are pulled outward, the connectors acting as rollers, and then the rotatory unit rotates around its center. Moreover, this process develops more rotatory units that interconnect through the linkages consisting of bars and joints. The design of the linking mechanism allows the arrayed units to operate simultaneously. Figure 1(c)(d) reveals that 2×2 units rotate in phase after force is applied.

The electrostatic driving force generated from the comb structure is related to the applied voltage, dielectric constant, the gap between two fingers, and the height and numbers of fingers. Since the dielectric constant regarding the medium (air) herein is essentially fixed, smaller gaps, greater height and more fingers are necessary for decreasing the voltage demand with large force. Corresponding to the design rule of the CMOS process, the gap could be as small as 0.8 μm. Meanwhile, this study develops a laminated structure [8] to meet the height requirement. By stacking the three metal and two oxide layers, the total height is raised to 5 μm. Additionally, this investigation designs three rows of comb structures to increase the number of fingers to sixty six pairs as shown in Fig. 2.

Slider-crank mechanism

For the practical devices, Fig. 3 illustrates the scanning electron micrography of the CMOS planar angular rotator, including single, 2×2 and 3×3 rotatory units. With the electrical potential, the comb structure will be pulled in the direction parallel to the capacitance plate. Additionally, the S-shape flexures join to the ends of the

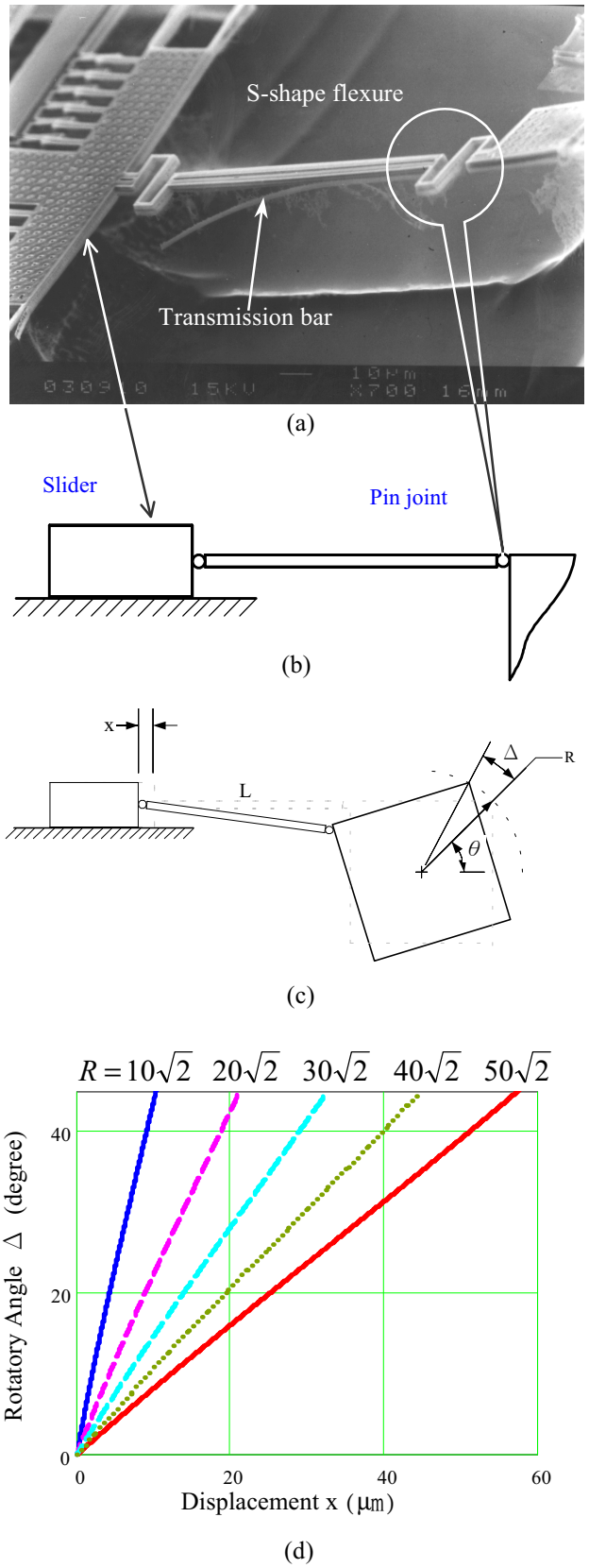

Figure 4. Slider-crank mechanism. (a)scanning electron micrograph, (b)equivalent model, (c)schematic diagram, and (d)plot of sliding distance and rotatory angle for different half diagonal length (R)

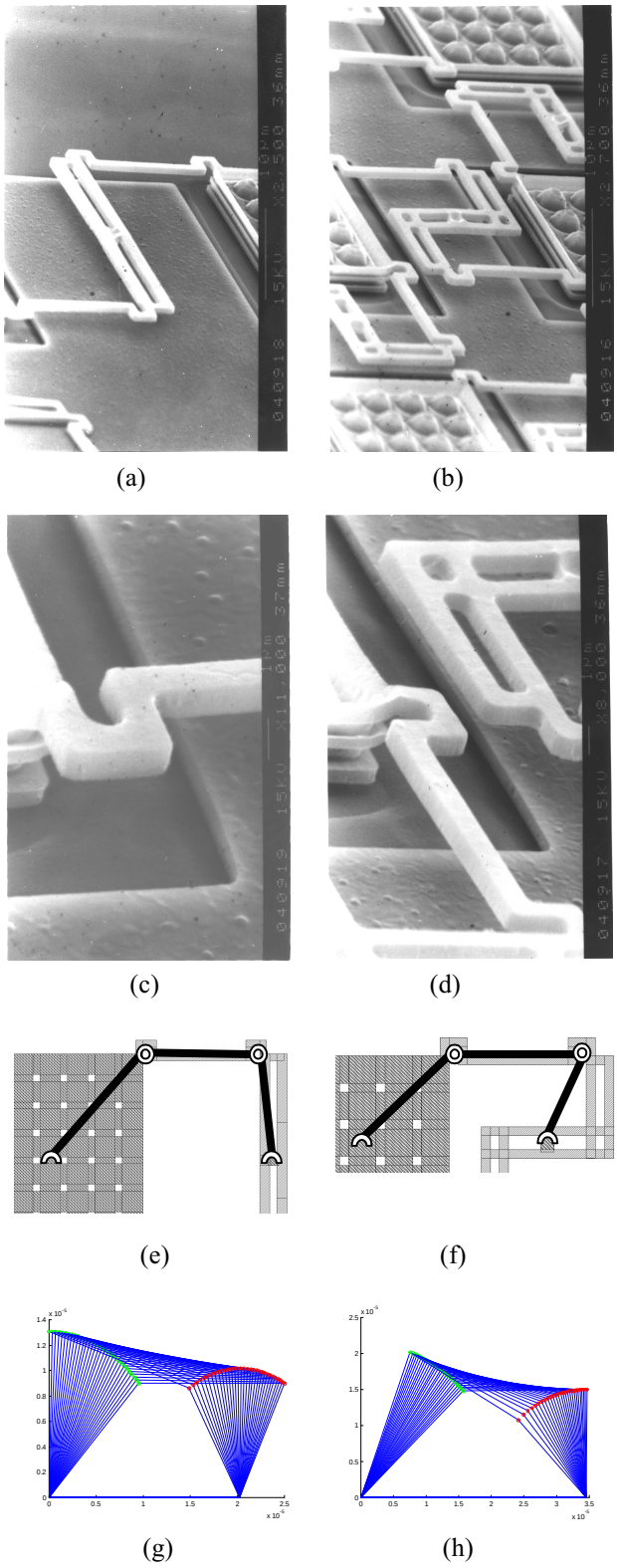

Figure 5. Four-bar linkage in the 2×2 and 3×3 rotatory units. (a)(b)oblique view, (c)(d) partial magnification, (e)(f)equivalent model, and (g)(h)plot of the stepping progress.

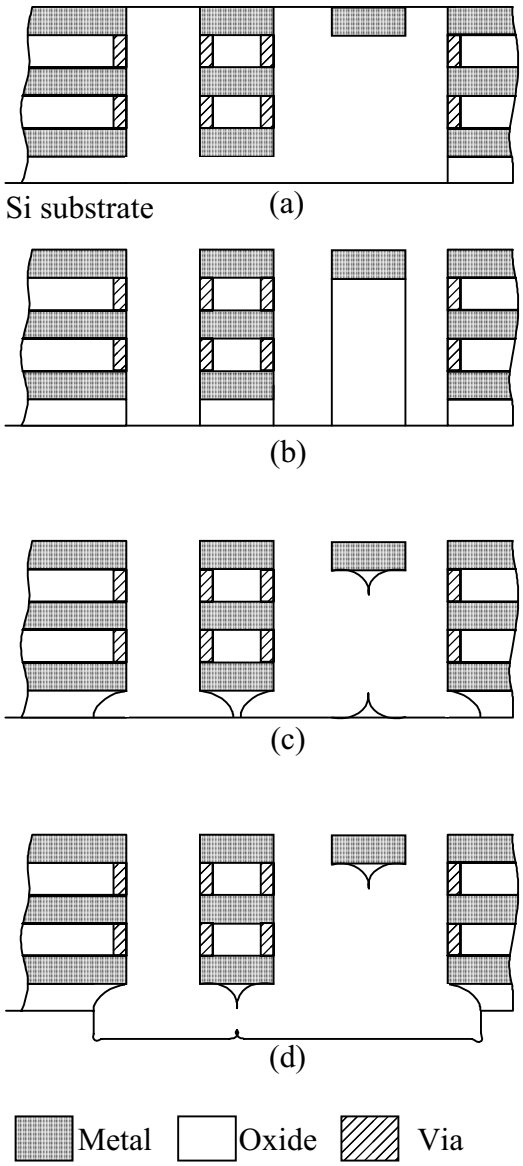

Figure 6. Schematic cross-section view of the post-CMOS process sequence. (a)following the CMOS foundry service, (b)anisotropic silicon dioxide etching, (c)isotropic silicon dioxide etching, (d)isotropic silicon etching.

transmission bar as depicted in Fig. 4(a)(b). Due to the flexures being thinner and softer than the transmission bar, the deformation would occur at the S-shape flexures and tilt the transmission bar. Subsequently, the rectilinear motion of the comb would be translated into the rotatory motion of the suspended unit via the transmission bar. The driving mechanism of the rotator, in sum, is a slider-crank system.

As Fig. 4(c) reveals, the relation between slider and crank includes sliding displacement, x and rotatory angle, Δ. The equation of motion [9] could be expressed as

$$x = R\left[\cos\theta - \cos(\theta+\Delta)\right] + \frac{R^2}{2L}\left[\sin(\theta+\Delta) - \sin\theta\right] \quad (1)$$

where θ is the initial angle from the horizontal, L is the length of the connecting rob, and R is the crank length. In the practical design, θ equals 45 degrees, L is the length of the transmission bar and equals 100 μm, and R is the half diagonal length of the suspended unit that represents the volume of the rotatory mass.

According to (1), the motion could be calculated and plotted with the various half diagonal lengths of the rotatory unit as in Fig. 4(d). The plot obviously reveals that more displacement is required for the larger unit at the same rotatory angle. To reduce the demand of actuating distance, this investigation suggests an array of small units, serving as a big unit.

Four-bar linkage

Besides single rotatory unit, 2×2 and 3×3 arrayed rotatory units are also presented (Fig. 3). Every unit interconnects by a mechanism equivalent to four-bar linkage, and, in doing so, each unit is driven simultaneously. As Fig. 5(e)(f) reveals, this research assumes the four joints are located at the center of the rotatory unit, the two flexures, and the center of the interconnected bar, respectively. Therefore, the motion of the interconnections resembles four-bar linkage, and the progress can be predicted as shown in Fig. 5(g)(h).

FABRICATION

The design of the planar angular rotator accords with the 0.6 μm SPTM (single poly and triple metal) foundry service of TSMC (Taiwan Semiconductor Manufacture Company). Following the foundry service, a simple post-process with maskless etching releases the structure. The post-process includes three steps to release the structure. Figure 6(a) presents the schematic cross-section view after the foundry service. All the passivation nitride is already removed and the metal layer is exposed. Although this violates the design rules that require the top metal layer to exist when the passivation nitride is absent, the process still works from the point of microfabrication. Figure 6(b) depicts the anisotropic oxide etching through to the silicon substrate by CF_4/O_2 RIE (reactive ion etching). Although most of the structure is constructed with the laminated layers, the soft parts are only defined by a single metal layer. Accordingly, isotropic silicon dioxide etching is needed to release the soft parts, as shown in Fig. 3.9(c), and this step could be completed by NF_3 RIE or concentrated HF (49%) wet etching [10]. Figure 3.9(d) shows the silicon substrate etching for releasing the whole structure. To employ the large undercut of the SF_6 RIE, 3 μm width of the beam could be released in twenty minutes by plasma etching. Furthermore, although a higher gas pressure can make the plasma etching more isotropic, when the pressure is too high the etching

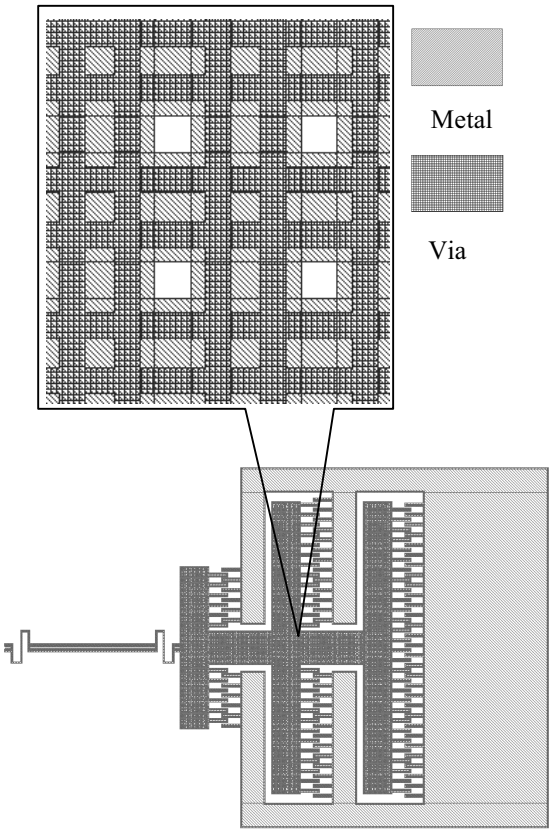

(a)

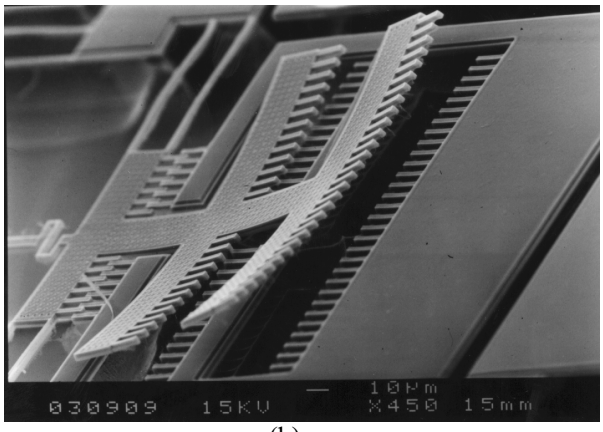

(b)

Figure 7. The effect of the layout of via. (a)layout of the comb structure, and (c)the free end of the structure bending out of plane.

depth becomes inconsistent.

RESULTS AND DISCUSSION

After the structure is fully released, the planar angular rotator could be driven obviously around 40 volts. However, most of the force was confined within the S-shape flexure and four-bar linkage, and the rotatory unit could not rotate more than 5 degrees. For improving the performance, a longer transmission bar and softer S-shape flexures would be necessary to satisfy the assumptions of pin-joint-like mechanism and, in doing so, make the motion smoother and larger.

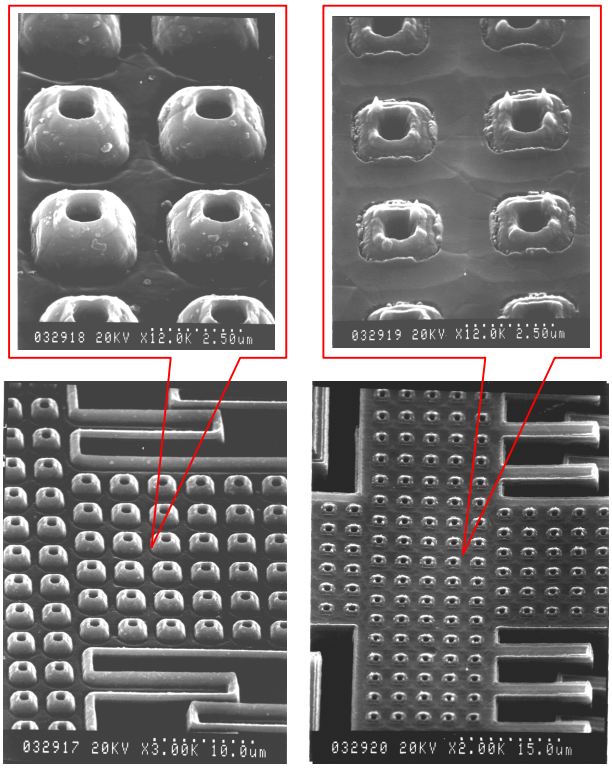

(a) (b)

Figure 8. Polymerization. (a)before etching, and (b)after etching with polymerization.

According to the CMOS foundry service adopted herein, the via implies that digging a tunnel in the oxide layer between the two metal layers, the upper metal layer fall down and present a concave profile after being deposited. According to Fig. 7(a), the layouts of the via not only exist in the boundary, but also cross each other in the center. In doing so, the metal layer would be rugged as shown in Fig. 8(a). However, the cave would be filled with polymer after F-based plasma etching (Fig. 8(b)). Restated, the polymerization would occur in the metal layer, accounting for why the metal layers is a good etching mask for plasma etching [11].

Using the via to connect each metal layer not only expands the electrode, but also protects the structure from the plasma etching (Fig. 6). However, with the rugged surface caused by the via, the free end of the structure would bend out-of-plane after being released, and the bending would cause more actuation rout to be required in the direction vertical to the substrate. In contrast, the flat surface without the layout of via would stray on plane after released.

CONCLUSION

This work has designed and fabricated the planar angular rotator using the CMOS process. Intelligent interconnections are used in arrayed rotators and the step progress is simulated as well. With the same actuating displacement, the arrayed units can achieve a larger rotatory angle. Experimentally, this study performs maskless etching with plasma or solvent and obtains excellent results including high selectivity and full release of the structure. Finally, the CMOS planar angular rotator could be driven by applying voltages of around 40 volts. The whole procedure is simple and compatible with the integrated circuits. This investigation not only reduces the developing time, but also minimizes the scale by following the advancing CMOS process.

ACKNOWLEDGEMENTS

This work was accomplished with much needed support and the authors wish to thank the following funding sources: Jennyi Chen, Chiyuan Lee, Hunghsuan Lin, Fuyuan Xiao, Tsungwei Huang, Shih-Chen Chang, Chunyuan Chi of the Institute of Applied Mechanics, National Taiwan University, for their valuable assistance in the experiment, and the National Chip Implementation Center is also appreciated.

REFERENCES

[1] M. Mehregany, S. D. Senturia, J. H. Lang, and P. Nagarkar, “Micromotor Fabrication,” *IEEE Trans. Electron Devices*, vol. 39, pp. 2060–2069, Sept. 1992.

[2] Yasseen, J. Mitchell, T. Streit, D. A. Smith, and M. Mehregany, “A Rotary Electrostatic Micromotor 1 ×8 Optical Switch,” *in Proc. IEEE 1996 11th Annu. Int. Workshop Micro-Electro-Mechanical Syst. (MEMS’98)*, Heidelberg, Germany, Jan. 25-29, 1998, pp. 116 -120.

[3] R. Legtenberg, E. Berenschot, M. Elwenspoek, and J. H. Fluitman, “Electrostatic Microactuators with Integrated Gear Linkages for Mechanical Power Transmission,” *in Proc. IEEE 1996 9th Annu. Int. Workshop Micro-Electro-Mechanical Syst. (MEMS’96)*, San Diego, CA, Jan. 11-15, 1996, pp. 204-209.

[4] J. J. Sniegowski and E. J. Garcia, “Surface-Micromachined Gear Train Driven by an On-Chip Electrostatic Microengine,” *IEEE Electron Device Lett.*, vol. 17, No. 7, July 1996, pp. 366-368.

[5] U. Beerschwinger, R. L. Reuben, and S. J., Yang, "Frictional Study of Micromotor Bearings," *Sensors and Actuators*, vol. A 63 , Dec. 1997, pp. 229-241.

[6] A. Horsley, M. B. Cohn, A. Singh, R. Horowitz, and A. P. Pisano, “Design and Fabrication of an Angular Microactuator for Magnetic Disk Drives,” *IEEE J. Microelectromechanical Syst.*, vol. 7, No. 2, June 1998, pp. 141-148.

[7] L. S. Fan, Y. C. Tai, and R. S. Muller, “Integrated Movable Micromechanical Structures for Sensors and Actuators,” *IEEE J. Microelectromechanical Syst.*, vol. 2, No. 1, Mar 1993, pp. 44-55.

[8] K. Fedder, S. Santhanam, M. L. Reed, S. C. Eagle, D. F. Gullou, M. S. –C. Lu, and L. R. Carley, “Laminated High-Aspect-Ratio Microstructures in A Conventional CMOS Process,” *in Proc. IEEE 1996 9th Annu. Int. Workshop Micro-Electro-Mechanical Syst. (MEMS’96)*, San Diego, CA, Jan. 11-15, 1996, pp. 13-18.

[9] G. H. Martin, *Kinematics and dynamics of machines*, McGraw-Hill, 2nd ed. , 1982, ch14.

[10] P. T. J. Gennissen and P. J. French, “Sacrificial Oxide Etching Compatible with Aluminum Metallization,” *in 9th Int. Conf. Solid-State Sensors and Actuators (TRANSDUCERS '97)*, Chicago, American, June 16-19, 1997, pp. 225-228.

[11] H. Jansen, H. Gardeniers, M. D. Boer, M. Elwenspoek,and J. Fluitman, "A Survey on the Reactive Ion Etching of Silicon in Microtechnology," *J. Micromech. Microeng.*, vol. 6, March 1996 pp. 14-28.